Published in final edited form as:
Mol Cancer Ther. 2014 July ; 13(7): 1750–1757. doi:10.1158/1535-7163.MCT-13-0930.

Metronomic docetaxel in PRINT® nanoparticles and EZH2 silencing have synergistic antitumor effect in ovarian cancer

Kshipra M. Gharpure[1,6], **Kevin S. Chu**[2], **Charles Bowerman**[2], **Takahito Miyake**[1], **Sunila Pradeep**[1], **Selanere L. Mangala**[3], **Hee-Dong Han**[1,3,8], **Rajesha Rupaimoole**[1,7], **Guillermo N. Armaiz-Pena**[1], **Tojan B. Rahhal**[2], **Sherry Y. Wu**[1], **J. Christopher Luft**[2], **Mary E Napier**[2], **Gabriel Lopez-Berestein**[3,4], **Joseph M DeSimone**[2], and **Anil K. Sood**[1,3,5]

[1]Department of Gynecology Oncology, The University of Texas MD Anderson Cancer Center (MDACC)

[2]Department of Chemistry, The University of North Carolina at Chapel Hill

[3]Center for RNA Interference and Non-Coding RNAs, MDACC

[4]Department of Experimental Therapeutics, MDACC

[5]Department of Cancer Biology, MDACC

[6]Experimental Therapeutics program, The University of Texas Graduate School of Biomedical Sciences at Houston

[7]Cancer Biology program, The University of Texas Graduate School of Biomedical Sciences at Houston

[8]Department of Immunology, School of Medicine, Konkuk University, South Korea

Abstract

The purpose of this study was to investigate the antitumor effects of a combination of metronomic doses of a novel delivery vehicle, PLGA-PRINT nanoparticles containing docetaxel, and anti-angiogenic mEZH2 siRNA incorporated into chitosan nanoparticles. *In vivo* dose-finding studies and therapeutic experiments were conducted in well-established orthotopic mouse models of epithelial ovarian cancer. Antitumor effects were determined on the basis of reduction in mean tumor weight and number of metastatic tumor nodules in the animals. The tumor tissues from these *in vivo* studies were stained to evaluate the proliferation index (Ki67), apoptosis index (cleaved caspase 3), and microvessel density (CD31). The lowest dose of metronomic regimen (0.5 mg/kg) resulted in significant reduction in tumor growth. The combination of PLGA-PRINT-docetaxel and CH-mEZH2 siRNA showed significant antitumor effects in the HeyA8 and SKOV3ip1 tumor models ($p<0.05$). Individual as well as combination therapies showed significant anti-angiogenic, anti-proliferative, and pro-apoptotic effects, and combination therapy

Correspondence to: Anil K. Sood, MD, 1155 Pressler St, Unit 1362, Houston, Texas 77030 (Phone: (713) 792-4130; FAX: (713) 792-7586; asood@mdanderson.org).

Conflict of interest- Joseph DeSimone is a founder, member of the board of directors, and maintains a financial interest in Liquidia Technologies. PRINT and Fluorocur are registered trademarks of Liquidia Technologies, Inc.

had additive effects. Metronomic delivery of PLGA-PRINT-docetaxel combined with CH-mEZH2 siRNA has significant antitumor activity in preclinical models of ovarian cancer.

Keywords

ovarian cancer; metronomic chemotherapy; PRINT particles; EZH2; chitosan

Introduction

Conventional chemotherapeutic regimens involve high doses of a cytotoxic agent followed by a 3- to 4-week rest period. Such scheduling was believed to be important to balance the drug's toxic effects on the tumor and on the host. However, recent studies using this approach have demonstrated a rapid acquisition of chemoresistance in certain patient populations after an initial response (1). Furthermore, conventional chemotherapy drugs have been associated with many toxic adverse effects that often impair quality of life and limit continuation of therapy (2).

Angiogenesis, or the formation of new blood vessels, has been shown to be vital for cancer growth and dissemination, thus making it an attractive target for anticancer therapies. Although standard chemotherapies target the highly proliferating cancer cells, they have little effect on the slowly dividing endothelial cells (2–4). In addition, the resting period between chemotherapy cycles allows the tumor endothelium to continue forming new vessels (2). However, the advent of metronomic dosing, which involves more frequent administration of low chemotherapeutic doses, has demonstrated the potential for more pronounced antitumor and anti-angiogenic effects than use of standard maximum tolerated dose (MTD) chemotherapy (5).

Particle replication in non-wetting templates (PRINT®) is a recently developed method of fabricating nanocarriers to efficiently deliver therapeutic moieties. This soft lithography process allows control of various parameters of the nanoparticles such as size, shape, and composition and thus allows more flexibility than do other approaches (6). Previous reports have shown that docetaxel incorporated in poly (lactic acid-co-glycolic acid) (PLGA)-PRINT nanoparticles has higher plasma exposure, greater intratumor accumulation than docetaxel alone (7).

Enhancer of Zeste Homolog 2 (EZH2), found to be overexpressed in tumor endothelial cells, methylates and inactivates vasohibin-1 (VASH1), a potent anti-angiogenic factor (8). We recently demonstrated that silencing EZH2 with siRNA incorporated into chitosan (CH) nanoparticles resulted in decreased angiogenesis and significant reduction in tumor growth (9). Here, we examined the biological effects of combined metronomic PLGA-PRINT-docetaxel and CH-mEZH2 siRNA in ovarian cancer models.

Methods

Cell lines and culture

HeyA8, SKOV3ip1 and HeyA8-luciferase cells were maintained as described previously (9). Briefly, the cells were maintained in 5% CO_2 at 37°C in RPMI-1640 media supplemented with 15% fetal bovine serum and 0.1% gentamycin sulfate. The cell lines were obtained from The American Type Cell Collection and were routinely tested for absence *Mycoplasma*.

Chitosan-mEZH2 siRNA

mEZH2-siRNA was incorporated into chitosan nanoparticles as described previously (8). The nanoparticles were formulated based on ionic gelation of anionic tripolyphosphate (TPP) and siRNA with cationic chitosan. Briefly, chitosan was dissolved in 0.25% acetic acid. The nanoparticles were spontaneously formed after adding TPP (0.25% w/v) and siRNA (1 μg/μL) to the chitosan solution under constant stirring at room temperature. The nanoparticles were then incubated at 4°C for 40 min and then centrifuged at 12,000 RPM for 40 min at 4°C. The pellet was washed three times to remove any unbound chemicals or siRNA. The nanoparticles thus formed were stored at 4°C until use.

PLGA-PRINT-docetaxel

PLGA-PRINT nanoparticles containing docetaxel were formulated as described previously (6). Briefly, 150 μl of 10 mg/ml PLGA and 10 mg/ml docetaxel were spread on a 6″ × 12″ sheet of poly (ethylene terephthalate) (PET) using a Mayer Rod (R. D. specialties). The solvent was evaporated with heat. The PET sheet was then placed in contact with the mold, and the mold was separated from the sheet by passing the mold and sheet through a hot laminator at 130°C and 80 psi (ChemInstruments Hot Roll Laminator). The mold was then placed in contact with another PET sheet coated with 2000 g/mol polyvinyl alcohol (PVOH). The nanoparticles were then transferred from the mold to the PET sheet by passing through a hot laminator and finally removed from the PET sheet by passing the sheet through rollers and applying water to dissolve the PVOH. The nanoparticles were purified and later concentrated by tangential flow filtration (Spectrum Labs).

Particle characterization

The nanoparticles were characterized with use of a scanning electron microscope (SEM). Briefly, a 50 μL nanoparticle sample was pipetted onto a glass slide. The sample was then dried and coated with a 3 nm thick gold palladium alloy using a Cressington 108 auto-sputter coater. Images were obtained with use of a Hitachi model S-4700 SEM at an accelerating voltage of 2 kV. Size and polydispersity index were measured by using dynamic light scattering (Malvern Instruments Nano-ZS).

Stability of PLGA-PRINT nanoparticles in plasma

Nanoparticles in phosphate bufferred saline were mixed with plasma at a 1:1 ratio and shaken at 37°C. At set time points, nanoparticles were removed and washed with water 20 times by tangential flow filtration to remove plasma proteins (mPES hollow fiber filter with

0.05 μm pore size, Spectrum Labs). The nanoparticles were then collected on a filter and imaged. The nanoparticles were imaged by SEM (Hitachi S-47000 Cold Cathode Field Emission Scanning Electron Microscope).

Drug loading

Docetaxel loading was measured with use of high performance liquid chromatography (HPLC) with C18 reverse phase column (Agilent Technology series 1200). All of the samples and standards of docetaxel and PLGA were prepared in acetonitrile. The nanoparticle samples were prepared by diluting a sample at a ratio of 1 to 10 in acetonitrile. A linear gradient of 100% water to 100% acetonitrile was run over for more than 10 min followed by 100% acetonitrile for 5 min. The flow rate was 1 mL/min, and the wavelength of detection was 205 nm.

In vitro drug release

We placed 100 μL of nanoparticle solution (200 μg/mL docetaxel) into a miniature dialysis unit with a 20 k MW cutoff. The solution was dialyzed against a constantly stirred 1 L bath of 1X PBS at 37°C. At each time point, the nanoparticle solution from each unit was removed and centrifuged. The nanoparticle pellet was analyzed for the amount of docetaxel remaining in the nanoparticles. By comparing this amount to the initial amount of docetaxel present in the system, the percentage of drug release could be calculated.

Orthotopic model of ovarian cancer

Female athymic nude mice were purchased from Taconic Farms and housed in pathogen-free conditions. They were cared for in accordance with the guidelines of the American Association for Accreditation of Laboratory Animal Care and the U.S. Public Health Service Policy on Human Care and Use of Laboratory Animals. All *in vivo* experiments and protocols were approved by MD Anderson's Institutional Animal Care and Use Committee.

For all of the *in vivo* experiments, cells were trypsinized at 60%-80% confluence, centrifuged at 1200 RPM for 6 min at 4°C, washed twice with phosphate-buffered saline (PBS), and reconstituted in Hanks balanced salt solution (HBSS) (Cellgro) to a desired concentration (1.5×10^6 cells/mL for HeyA8 and 5×10^6 cells/mL for SKOV3ip1 for intraperitoneal injections). For intraovarian injections, HeyA8-luciferase cells (1.5×10^6cells/mL) were resuspended in 1:1 mixture of BD matrigel and HBSS). Mice were anesthetized with ketamine and an incision was made just above the left ovary. A 1mL tuberculin syringe with a 30-gauge needle was used to inject cells directly into the ovary. The incision was then closed using surgical clips. The mice were returned to cages until full recovery. The clips were removed after a week when the incision was fully healed.

The dose-finding studies for PLGA-PRINT-docetaxel were performed with five treatment groups (10 mice/group) divided into a control (saline) group, maximum tolerated dose (MTD- 20 mg/kg) group, and three groups at 0.5, 1.0, and 2.0 mg/kg of docetaxel injections. Each mouse was injected intraperitoneally (i.p.) with 200 μL of cell suspension containing 3×10^5 HeyA8 cells. Treatment was started 1 week after the injections of tumor cells. A MTD dose of 20 mg/kg was given once in 2 weeks during the entire *in vivo* treatment. Saline and

metronomic doses of docetaxel were given as 200 μL i.p. injections three times per week. The mice were monitored daily for any signs of toxic adverse effects. All the mice were sacrificed when the mice in any group seemed to be moribund. Mouse weight, tumor weight and the number of nodules were recorded.

For the therapeutic experiment, mice were divided into four groups (10 mice/group): CH-control siRNA, CH-mEZH2 siRNA, PLGA-PRINT-docetaxel, and a combination of PLGA-PRINT-docetaxel and CH-mEZH2 siRNA. The mice were injected i.p. with a 200 μL cell suspension of either HeyA8 (3×10^5 cells/mouse) or SKOV3ip1 cells (1×10^6 cells/mouse). Treatment was started 1 week after the tumor cell injections. The siRNA was injected at a dose of 3.5 μg in 100 μL of saline intravenously (i.v.) twice weekly. The PLGA-PRINT-docetaxel was injected at a dose of 0.5 mg/kg in 125 μL of saline i.p. three times weekly. The mice were sacrificed when the mice in any group became moribund. Mouse weight, tumor weight, and the number of tumor nodules were recorded. Tumors were collected and the tissues were formalin-fixed or snap-frozen in optimal cutting medium for immunohistochemical staining.

We performed additional therapeutic experiment with HeyA8-luciferese intraovarian mouse model. The mice were injected with 100 μL suspension of HeyA8 cells (3×10^5 cells/mouse). The mice were treated as mentioned earlier. Bioluminescence imaging was conducted to monitor metastasis after initiation of treatments. Imaging and data acquisition were performed with IVIS spectrum system coupled to the Living Image Software (Xenogen, Alameda, CA). The mice were anesthetized in an acrylic chamber with a mixture of 1% isoflurane in air. They were then injected intraperitoneally with luciferin potassium salt (15 mg/mL) in PBS at a dose of 150 mg/kg body weight. A digital grayscale image was initially acquired which was then overlaid with a pseudocolor image representing the spatial distribution of detected photons emerging from active luciferase present within the animal. Signal intensity was expressed as a sum of all photons detected per second.

Immunohistochemical staining

For immunohistochemical analysis, paraffin sections (5 μm) of tumor tissues were sectioned and used for the detection of a proliferation marker (Ki67) and an apoptosis marker (cleaved caspase 3). Frozen sections were used to detect the expression of an endothelial cell marker (CD31). Formalin-fixed paraffin sections were deparaffinized by sequential washing with xylene, 100% ethanol, 95% ethanol, 80% ethanol, and PBS. A suitable antigen retrieval method was used. For CD31 staining, frozen cut sections were fixed by incubating for 5 min in cold acetone, acetone + chloroform (1:1), and then cold acetone in a sequential manner. No antigen retrieval procedure was necessary for CD31 staining. For all of the slides, endogenous peroxide was blocked by incubating the slides with 3% hydrogen peroxide in PBS. To prevent nonspecific binding of the primary antibody, the slides were incubated in 5% normal horse serum + 1% normal goat serum (for Ki67 and CD31 staining) or in 4% fish gelatin in PBS (for cleaved caspase 3 staining) This was followed by an overnight incubation at 4°C with a primary antibody diluted in the protein block solution. The primary antibodies used were Ki67-rabbit polyclonal anti-human antibody from Thermo/lab vision, cleaved caspase 3-rabbit polyclonal anti-human, mouse, rat from Biocare Medical, and

CD31 rat anti-mouse antibody from Pharmingen/Invitrogen. After the slides were incubated with primary antibodies, they were washed with PBS and incubated with suitable secondary antibodies. For Ki67 and CD31 staining, goat anti-rabbit HRP antibody diluted in protein block solution was used, and the slides were incubated in this solution for 1 h at room temperature. For cleaved caspase 3 staining, the slides were first incubated with biotinylated 4+ goat anti-rabbit secondary antibody for 20 min, after which they were washed with PBS and later incubated with streptavidin 4+ goat anti-rabbit secondary antibody for 20 min. After the slides were incubated with secondary antibody, they were washed with PBS followed by development with DAB (Research Genetics). The nuclei were stained with Gill's hematoxylin solution, and the slides were then mounted with paramount mounting media.

For Ki67 and cleaved caspase staining, the number of tumor cells that were positive for expression were counted. For CD31 staining, microvessel-like structures containing endothelial cells that were positive for CD31 staining were counted. Expression was quantified by using 15 random fields of slides at 100× magnification.

Statistical analysis

Continuous variables were analyzed with use of the Student's t test or the Mann-Whiney U test. A p value less than 0.05 was considered to be significant.

Results

PLGA-PRINT nanoparticle characterization

Before carrying out *in vivo* experiments, we first examined the PRINT nanoparticles, which were of uniform size (80 × 320 nm) and shape as shown in Figure 1A. The percent docetaxel loading, calculated by HPLC, was 17.1% (Figure 1B). When incubated with plasma, the nanoparticles were stable up to 3 days (Figure 1C). The nanoparticles exhibited a "burst release profile," in which 100% of the drug is released within 24 hours (Figure 1D). We performed cell viability experiments after incubation with PLGA-PRINT-nanoparticles. There was no effect on cell viability after incubation with PRINT nanoparticles (data not shown). We also conducted stability assays of the nanoparticles. The nanoparticles were stable at −20°C up to 3 months while the lyophilized nanoparticles were stable at 4°C up to 6 months (Supplementary Table 1).

Internalization and stability assays of chitosan nanoparticles

We evaluated intracellular delivery of chitosan nanoparticles using HeyA8 cells and Cy3 labeled CH-control siRNA. There was efficient internalization of these nanoparticles into the cancer cells (Supplementary Figure 1A). We also checked the stability of CH-mEZH2 siRNA in presence of 10% FBS. Naked siRNA was degraded rapidly upon incubation with serum while siRNA protected by chitosan nanoparticles was not degraded (Supplementary Figure 1B). To evaluate for any possible effects of the nanoparticles alone, we tested the effect of chitosan nanoparticles on SKOV3ip1 cells. There was no effect on cell viability after 48 hours of incubation with chitosan nanoparticles (Supplementary Figure 1C).

Determining the optimal metronomic dose for PLGA-PRINT-docetaxel nanoparticles

Next, we conducted a dose-finding study to determine the lowest docetaxel dose that is biologically effective. All of the doses were significantly effective in reducing the tumor burden ($p<0.05$ for MTD and $p<0.01$ for metronomic doses). The lowest dose at 0.5 mg/kg reduced the tumor weight by approximately 80% and was, therefore, chosen for subsequent therapeutic studies (Figure 2A).

Therapeutic studies with metronomic doses

We next determined whether a combination of PLGA-PRINT-docetaxel nanoparticles with CH-mEZH2 siRNA would result in a strong antitumor effect. The mice were divided into the following groups: (a) CH-control siRNA, (b) CH-mEZH2 siRNA, (c) metronomic dose of PLGA-PRINT-docetaxel (0.5 mg/kg), and (d) metronomic dose of PLGA-PRINT-docetaxel and CH-mEZH2 siRNA. PLGA-PRINT-docetaxel was injected i.p. three times weekly, whereas siRNA was injected i.v. twice weekly. CH-mEZH2 siRNA treatment reduced aggregate tumor weight by approximately 70% in both HeyA8 and SKOV3ip1 models ($p<0.01$ for HeyA8 and $p<0.05$ for SKOV3ip1). PLGA-PRINT-docetaxel treatment reduced tumor weight by ~80% ($p<0.01$). Combination therapy showed the greatest therapeutic benefit with ~95% reduction in tumor weight in both models ($p<0.001$ in HeyA8 and $p<0.01$ in SKOV3 ip1). In the HeyA8 model, individual therapies resulted in reduction in the number of nodules, and combination therapy showed a significant effect ($p<0.01$). In the SKOV3ip1 model, combination therapy as well as individual therapies resulted in significant reduction of tumor nodules ($p<0.05$) (Figures 2B and 2C). For the objective evaluation of reduction of metastasis, we conducted an additional *in vivo* experiment with luciferase labeled HeyA8 cells injected directly into the ovary. Bioluminescence imaging revealed reduced metastasis after individual and combination therapies (Figures 3A and 3B). No significant effects of therapy were noted on mouse weight or activity. Following siRNA delivery, downregulation of murine EZH2 in endothelial cells was confirmed at mRNA level by qRT-PCR and at protein level by immunohistochemistry (Supplementary Figures 1D and 1E).

Biological effects of metronomic PLGA-PRINT-docetaxel and CH-mEZH2 siRNA therapy

To determine the biological effects of combined therapy, *in vivo* samples were subjected to immunohistochemical analysis for Ki67, cleaved caspase 3, and CD31 (Figure 3C). Individual as well as combination therapies resulted in a significant reduction in proliferation ($p<0.001$). Individual metronomic dosing of PLGA-PRINT-docetaxel and CH-mEZH2 siRNA increased the apoptotic index significantly ($p<0.05$), whereas the combination therapy had an additive effect ($p<0.001$). Previous studies have suggested that metronomic chemotherapy affects endothelial cell proliferation. To test this hypothesis, frozen tumor sections from the *in vivo* studies were stained for CD31. CH-mEZH2 siRNA as well as metronomic PLGA-PRINT-docetaxel therapy showed a significant effect on tumor vasculature ($p<0.01$). Combining CH-mEZH2 siRNA with metronomic docetaxel also resulted in a significant reduction in microvessel density ($p<0.01$).

Discussion

The key finding from this study is the pronounced antitumor effect of metronomic delivery of PLGA-PRINT-docetaxel therapy along with CH-mEZH2 siRNA. We have previously shown that the major biological effect of metronomic therapy is through its anti-angiogenic effects (8, 10). Concordant with those studies, we saw a significant anti-angiogenic effect and downstream anti-proliferative and pro-apoptotic effects.

Metronomic chemotherapy has been proposed to serve as an alternative to the standard dosing schedule to overcome the problems associated with the latter. Long-term administration of standard chemotherapies is limited by their toxic effects on normal cells, whereas metronomic therapy has minimal adverse effects (2–5, 11). Metronomic dosing has also been shown to be effective against chemoresistant models (12, 13). Whereas standard therapy has little effect on tumor vasculature, studies have shown that metronomic therapy has significant anti-angiogenic effects (2–5, 11–14). Our findings from this study also suggest that endothelial cells are quite sensitive to low doses of docetaxel therapy in a metronomic schedule. Moreover, the low toxicity profile of metronomic dosing makes it a suitable candidate for combination therapies. Several studies have demonstrated that a combination of metronomic dosing with an anti-angiogenic therapy has significant anti-tumor effects in ovarian cancer (10, 13, 15, 16). Here, we provide strong evidence that metronomic docetaxel dosing with novel PRINT nanoparticles has strong anti-proliferative, anti-apoptotic, and anti-angiogenic effects and that combining it with CH-mEZH2 siRNA proved to be highly efficacious in reducing tumor burden.

Angiogenesis is one of the key processes that promotes cancer growth and metastasis. The process is regulated by several pro and anti-angiogenic factors in the body that become deregulated in cancer (17). EZH2 was found to be overexpressed in tumor-associated endothelial cells (8). Previous studies in our laboratory (9) have shown that VEGF directly increases EZH2 expression on endothelial cells, which in turn methylates and inhibits an anti-angiogenic factor, vasohibin-1 (VASH1). Several other studies have shown that EZH2 plays a critical role in several oncogenic pathways (18–21). Hence, silencing EZH2 in endothelial cells is a promising therapeutic approach to target angiogenesis.

With increasing understanding of toxicity profiles and because of the poor pharmacokinetic properties of the current chemotherapeutics, there is a need to develop a delivery vehicle with improved drug efficacy and reduced toxicity. Docetaxel is a commonly used chemotherapeutic agent but is often associated with systemic toxicities. When compared with docetaxel alone, PLGA-PRINT nanoparticles loaded with docetaxel showed higher plasma exposure, higher tumor concentration and lower volume of distribution in a subcutaneous ovarian cancer mouse model (6). It also exhibited a characteristic “burst release profile,” in which 100% of the drug is released within 24 hours. This property is ideal for metronomic drug delivery.

In summary, we have demonstrated that combination therapy of metronomic PLGA-PRINT-docetaxel and CH-mEZH2siRNA is highly effective in reducing tumor burden. This approach holds great potential for new treatment strategies for ovarian and other cancers.

Supplementary Material

Refer to Web version on PubMed Central for supplementary material.

Acknowledgments

Financial Information

K.G. is supported by Altaman Goldstein Discovery Fellowship. S.Y.W. is supported by Ovarian Cancer Research Fund, Foundation for Women's Cancer, and Cancer Prevention Research Institute of Texas training grants (RP101502, RP101489 and RP110595). Portions of this work were supported by the NIH (U54 CA151668, CA016672, CA109298, P50 CA083639, P50 CA098258, and UH2 TR000943-01), the DOD (OC120547 and OC093416), the Ovarian Cancer Research Fund (Program Project Development Grant), the Blanton-Davis Ovarian Cancer Research Program, Meyer and Ida Gordon Foundation #2, the RGK Foundation, the Gilder Foundation, and the Betty Anne Asche Murray Distinguished Professorship.

We thank D. Reynolds and Dr. R. Langley for technical assistance and helpful discussions.

References

1. Agarwal R, Kaye SB. Ovarian cancer: strategies for overcoming resistance to chemotherapy. Nat Rev Cancer. 2003; 3:502–16. [PubMed: 12835670]
2. Gasparini G. Metronomic scheduling: the future of chemotherapy? The Lancet Oncology. 2001; 2:733–40. [PubMed: 11902515]
3. Hanahan D, Bergers G, Bergsland E. Less is more, regularly: metronomic dosing of cytotoxic drugs can target tumor angiogenesis in mice. The Journal of Clinical Investigation. 2000; 105:1045–7. [PubMed: 10772648]
4. Kerbel RS, Kamen BA. The anti-angiogenic basis of metronomic chemotherapy. Nat Rev Cancer. 2004; 4:423–36. [PubMed: 15170445]
5. Romiti A, Cox MC, Sarcina I, Rocco R, D'Antonio C, Barucca V, et al. Metronomic chemotherapy for cancer treatment: a decade of clinical studies. Cancer Chemotherapy and Pharmacology. 2013; 72:13–33. [PubMed: 23475105]
6. Enlow EM, Luft JC, Napier ME, DeSimone JM. Potent engineered PLGA nanoparticles by virtue of exceptionally high chemotherapeutic loadings. Nano Lett. 2011; 11:808–13. [PubMed: 21265552]
7. Chu KS, Hasan W, Rawal S, Walsh MD, Enlow EM, Luft JC, et al. Plasma, tumor and tissue pharmacokinetics of Docetaxel delivered via nanoparticles of different sizes and shapes in mice bearing SKOV-3 human ovarian carcinoma xenograft. Nanomedicine. 2013; 9:686–93. [PubMed: 23219874]
8. Lu C, Bonome T, Li Y, Kamat AA, Han LY, Schmandt R, et al. Gene Alterations Identified by Expression Profiling in Tumor-Associated Endothelial Cells from Invasive Ovarian Carcinoma. Cancer Research. 2007; 67:1757–68. [PubMed: 17308118]
9. Lu C, Han HD, Mangala LS, Ali-Fehmi R, Newton CS, Ozbun L, et al. Regulation of tumor angiogenesis by EZH2. Cancer Cell. 2010; 18:185–97. [PubMed: 20708159]
10. Merritt WM, Nick AM, Carroll AR, Lu C, Matsuo K, Dumble M, et al. Bridging the Gap between Cytotoxic and Biologic Therapy with Metronomic Topotecan and Pazopanib in Ovarian Cancer. Molecular Cancer Therapeutics. 2010; 9:985–95. [PubMed: 20371710]
11. Klement G, Baruchel S, Rak J, Man S, Clark K, Hicklin DJ, et al. Continuous low-dose therapy with vinblastine and VEGF receptor-2 antibody induces sustained tumor regression without overt toxicity. J Clin Invest. 2000; 105:R15–24. [PubMed: 10772661]
12. Browder T, Butterfield CE, Kraling BM, Shi B, Marshall B, O'Reilly MS, et al. Antiangiogenic scheduling of chemotherapy improves efficacy against experimental drug-resistant cancer. Cancer Res. 2000; 60:1878–86. [PubMed: 10766175]
13. Kamat AA, Kim TJ, Landen CN Jr, Lu C, Han LY, Lin YG, et al. Metronomic chemotherapy enhances the efficacy of antivascular therapy in ovarian cancer. Cancer Res. 2007; 67:281–8. [PubMed: 17210709]

14. Merritt WM, Danes CG, Shahzad MMK, Lin YG, Kamat AA, Han LY, et al. Anti-angiogenic properties of metronomic topotecan in ovarian carcinoma. Cancer Biology & Therapy. 2009; 8:1596–603. [PubMed: 19738426]

15. Aigner J, Bischofs E, Hallscheidt P, Sohn C, Schneeweiss A, Eichbaum M. Long-term remission in a patient with heavily pretreated, advanced ovarian cancer achieved by bevacizumab and metronomic cyclophosphamide treatment. Anticancer Drugs. 2011; 22:1030–3. [PubMed: 21970854]

16. Hashimoto K, Man S, Xu P, Cruz-Munoz W, Tang T, Kumar R, et al. Potent preclinical impact of metronomic low-dose oral topotecan combined with the antiangiogenic drug pazopanib for the treatment of ovarian cancer. Mol Cancer Ther. 2010; 9:996–1006. [PubMed: 20371722]

17. Folkman J. What Is the Evidence That Tumors Are Angiogenesis Dependent? Journal of the National Cancer Institute. 1990; 82:4–7. [PubMed: 1688381]

18. Guo J, Cai J, Yu L, Tang H, Chen C, Wang Z. EZH2 regulates expression of p57 and contributes to progression of ovarian cancer in vitro and in vivo. Cancer Science. 2011; 102:530–9. [PubMed: 21205084]

19. Rao Z-Y, Cai M-Y, Yang G-F, He L-R, Mai S-J, Hua W-F, et al. EZH2 supports ovarian carcinoma cell invasion and/or metastasis via regulation of TGF-β1 and is a predictor of outcome in ovarian carcinoma patients. Carcinogenesis. 2010; 31:1576–83. [PubMed: 20668008]

20. Seward S, Semaan A, Qazi AM, Gruzdyn OV, Chamala S, Bryant CC, et al. EZH2 blockade by RNA interference inhibits growth of ovarian cancer by facilitating re-expression of p21waf1/cip1 and by inhibiting mutant p53. Cancer letters. 2013; 336:53–60. [PubMed: 23603558]

21. Tsang DPF, Cheng ASL. Epigenetic regulation of signaling pathways in cancer: Role of the histone methyltransferase EZH2. Journal of Gastroenterology and Hepatology. 2011; 26:19–27. [PubMed: 21175789]

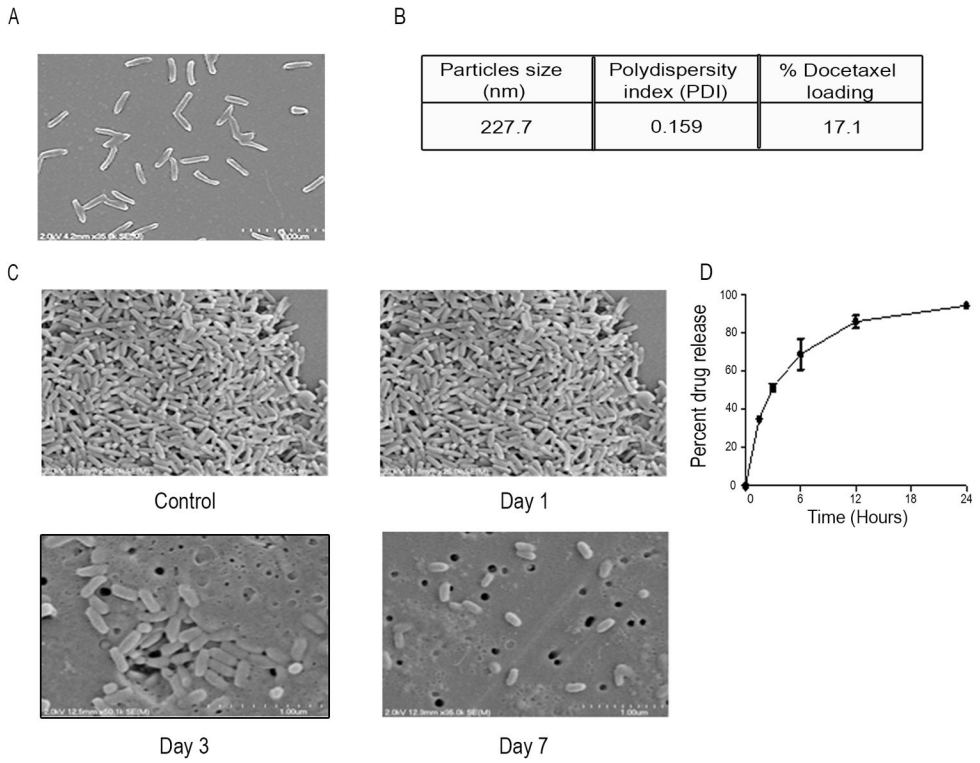

Figure 1.

Particle characterization, drug loading and release profile: (A) 80 × 320 nm PLGA-PRINT-docetaxel nanoparticles- Scanning electron microscopy (SEM) image. (B) Size, PDI and drug loading profile. (C) Stability of PLGA-PRINT nanoparticles after incubation with plasma. SEM images are shown. Nanoarticles before (top left panel) and after (top right panel) plasma exposure for 1 day. Nanoparticles after 3 days in plasma (Bottom left panel). Nanoparticles after 7 days in plasma (Bottom right panel). (D) *In vitro* drug release profile.

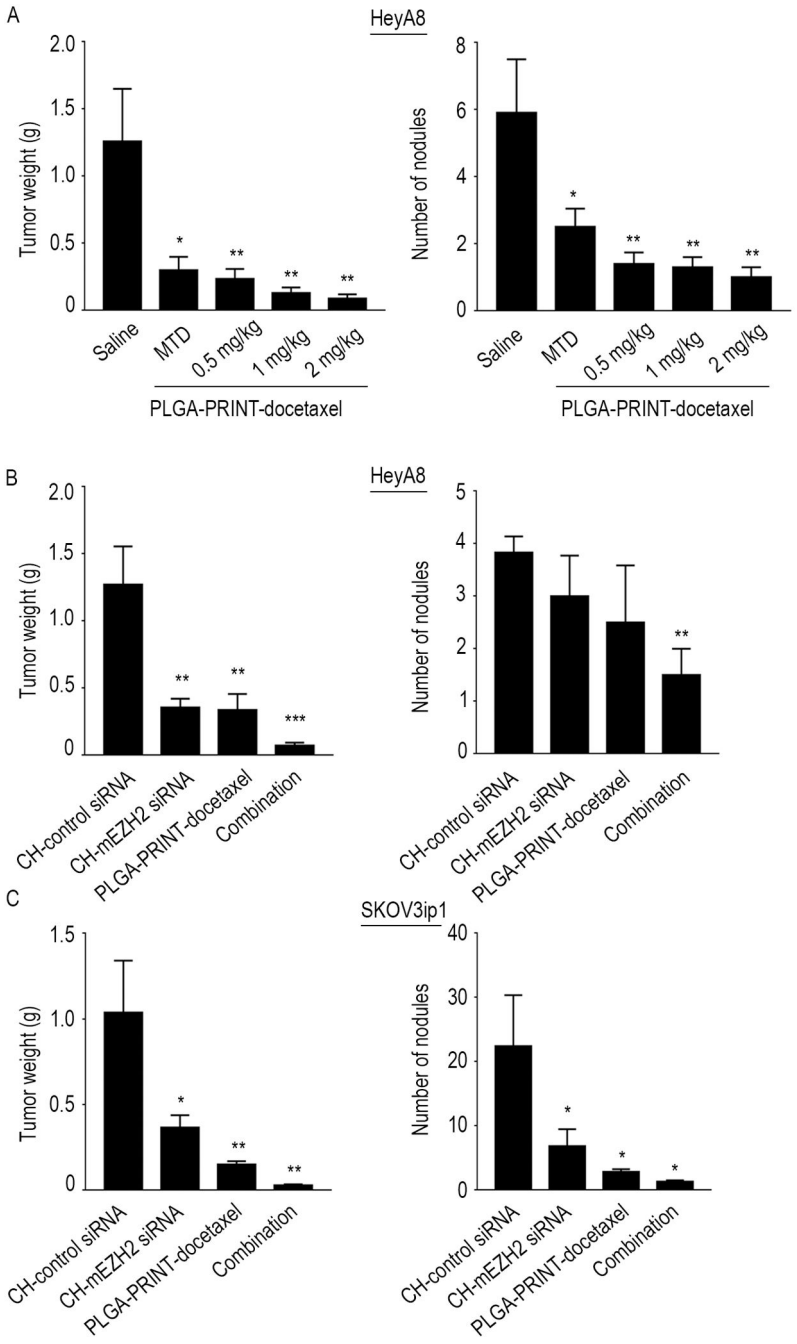

Figure 2.

Dose determination and therapeutic *in vivo* experiments: (A) Dose finding study: Effect of metronomic (0.5, 1, 2 mg/kg) versus MTD doses (20 mg/kg) of PLGA-PRINT-docetaxel therapy on HeyA8 orthotopic mouse model. Average of tumor weight and number of nodules are shown. All the metronomic doses showed significant tumor reduction. Error bars represent S.E.M. *p<0.05, **p<0.01 compared to saline. Tumor growth inhibition with CH-mEZH2 siRNA and PLGA-PRINT-docetaxel, alone and with combination therapy in HeyA8 (B) and SKOV3ip1 (C) orthotopic mouse model. Average of tumor weights and

number of nodules are shown. Combination therapy showed the greatest therapeutic benefit in both mouse models. There was significant reduction in tumor weight as well as in tumor nodules. Error bars represent S.E.M. *p<0.05, **p<0.01, ***p<0.001 compared to CH-control siRNA group.

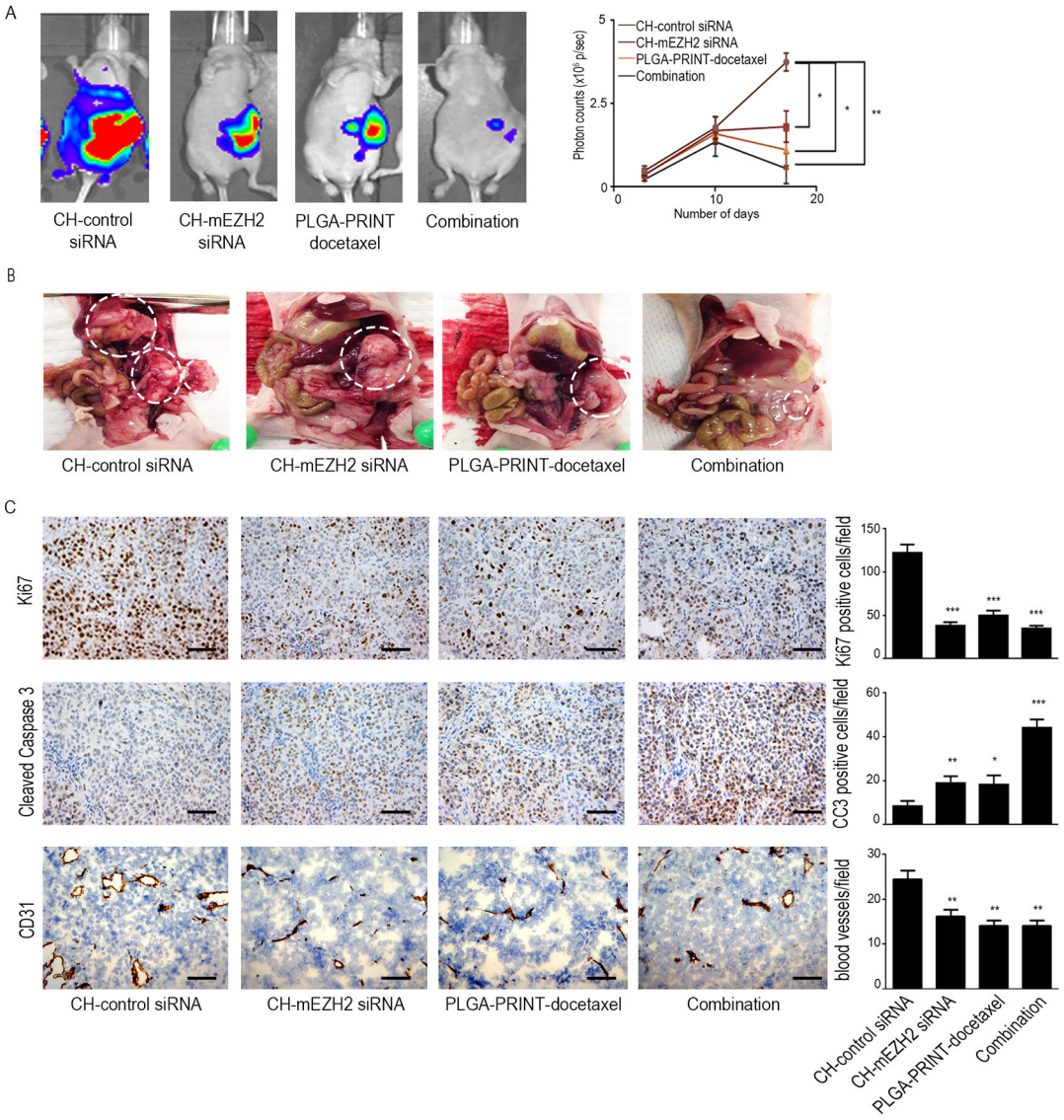

Figure 3.

Biologicals effects of the treatments: (A) Noninvasive images of metastasis and tumor growth in orthotopic mouse model of HeyA8. Representative images show reduction in metastasis after the treatment of CH-mEZH2 siRNA, PLGA-PRINT-docetaxel and combination therapy. The effect is pronounced in the combination group. Quantification of luciferin signal intensity is shown in the adjoining graph. Error bars represent S.E.M. *p<0.05, **p<0.01. (B) Representative images of sites of metastasis and tumor burden in orthotopic mouse model of HeyA8. The data shows reduction in metastasis after individual and combination therapies. (C) Proliferation index (Ki67), apoptosis index (cleaved caspase 3) and microvessel density (CD31) in HeyA8 tumors treated with CH-control siRNA, CH-mEZH2 siRNA, PLGA-PRINT-docetaxel and combination therapy. A graphic representation of the average number of Ki67 or cleaved caspase 3 positive cells and CD31 positive vessels are shown in the adjoining graphs. Combination therapy showed significant anti-proliferative, pro-apoptotic and anti-angiogenic effects. Error bars represent S.E.M.

*p<0.05, **p<0.01, ***p<0.001 compared to CH-control siRNA group. The scale bar represents 100 μm.